

PDF hosted at the Radboud Repository of the Radboud University Nijmegen

The following full text is a preprint version which may differ from the publisher's version.

For additional information about this publication click this link.

<http://hdl.handle.net/2066/124596>

Please be advised that this information was generated on 2021-09-21 and may be subject to change.

Observation of Υ production in hadronic Z^0 decays

The OPAL Collaboration

Abstract

Evidence for the production of Υ mesons in hadronic Z^0 decays is presented. Using a sample of 3.7 million hadronic events, eight Υ candidates are identified from their decays into e^+e^- and $\mu^+\mu^-$ pairs. The estimated background in the signal region is 1.6 ± 0.3 events. Based on existing theoretical models for inclusive Υ production, where Υ is one of the three lightest Υ states, the following branching ratio is obtained:

$$Br(Z^0 \rightarrow \Upsilon + X) = (1.0 \pm 0.4 \pm 0.1 \pm 0.2) \times 10^{-4},$$

where the first error is statistical, the second systematic and the third error accounts for uncertainties in the production mechanism.

(Submitted to Phys. Lett. B)

The OPAL Collaboration

G. Alexander²³, J. Allison¹⁶, N. Altekamp⁵, K. Ametewee²⁵, K.J. Anderson⁹, S. Anderson¹², S. Arcelli², S. Asai²⁴, D. Axen²⁹, G. Azuelos^{18,a}, A.H. Ball¹⁷, E. Barberio²⁶, R.J. Barlow¹⁶, R. Bartoldus³, J.R. Batley⁵, G. Beaudoin¹⁸, J. Bechtluft¹⁴, G.A. Beck¹³, C. Beeston¹⁶, T. Behnke⁸, A.N. Bell¹, K.W. Bell²⁰, G. Bella²³, S. Bentvelsen⁸, P. Berlich¹⁰, S. Bethke¹⁴, O. Biebel¹⁴, I.J. Bloodworth¹, J.E. Bloomer¹, P. Bock¹¹, H.M. Bosch¹¹, M. Boutemour¹⁸, B.T. Bouwens¹², S. Braibant¹², P. Bright-Thomas²⁵, R.M. Brown²⁰, H.J. Burckhart⁸, C. Burgard²⁷, R. Bürigin¹⁰, P. Capiluppi², R.K. Carnegie⁶, A.A. Carter¹³, J.R. Carter⁵, C.Y. Chang¹⁷, C. Charlesworth⁶, D.G. Charlton^{1,b}, D. Chrisman⁴, S.L. Chu⁴, P.E.L. Clarke¹⁵, S.G. Clowes¹⁶, I. Cohen²³, J.E. Conboy¹⁵, O.C. Cooke¹⁶, M. Cuffiani², S. Dado²², C. Dallapiccola¹⁷, G.M. Dallavalle², C. Darling³¹, S. De Jong¹², L.A. del Pozo⁸, M.S. Dixit⁷, E. do Couto e Silva¹², E. Duchovni²⁶, G. Duckeck⁸, I.P. Duerdoth¹⁶, U.C. Dunwoody⁸, J.E.G. Edwards¹⁶, P.G. Estabrooks⁶, H.G. Evans⁹, F. Fabbri², B. Fabbro²¹, P. Fath¹¹, F. Fiedler¹², M. Fierro², M. Fincke-Keeler²⁸, H.M. Fischer³, R. Folman²⁶, D.G. Fong¹⁷, M. Foucher¹⁷, H. Fukui²⁴, A. Fürtjes⁸, P. Gagnon⁷, A. Gaidot²¹, J.W. Gary⁴, J. Gascon¹⁸, S.M. Gascon-Shotkin¹⁷, N.I. Geddes²⁰, C. Geich-Gimbel³, S.W. Gensler⁹, F.X. Gentit²¹, T. Gerasis²⁰, G. Giacomelli², P. Giacomelli⁴, R. Giacomelli², V. Gibson⁵, W.R. Gibson¹³, D.M. Gingrich^{30,a}, J. Goldberg²², M.J. Goodrick⁵, W. Gorn⁴, C. Grandi², E. Gross²⁶, C. Hajdu³², G.G. Hanson¹², M. Hansroul⁸, M. Hapke¹³, C.K. Hargrove⁷, P.A. Hart⁹, C. Hartmann³, M. Hauschild⁸, C.M. Hawkes⁸, R. Hawkings⁸, R.J. Hemingway⁶, G. Herten¹⁰, R.D. Heuer⁸, M.D. Hildreth⁸, J.C. Hill⁵, S.J. Hillier⁸, T. Hilse¹⁰, P.R. Hobson²⁵, D. Hochman²⁶, R.J. Homer¹, A.K. Honma^{28,a}, D. Horváth^{32,c}, R. Howard²⁹, R.E. Hughes-Jones¹⁶, D.E. Hutchcroft⁵, P. Igo-Kemenes¹¹, D.C. Imrie²⁵, A. Jawahery¹⁷, P.W. Jeffreys²⁰, H. Jeremie¹⁸, M. Jimack¹, A. Joly¹⁸, M. Jones⁶, R.W.L. Jones⁸, U. Jost¹¹, P. Jovanovic¹, D. Karlen⁶, T. Kawamoto²⁴, R.K. Keeler²⁸, R.G. Kellogg¹⁷, B.W. Kennedy²⁰, B.J. King⁸, J. King¹³, J. Kirk²⁹, S. Kluth⁵, T. Kobayashi²⁴, M. Kobel¹⁰, D.S. Koetke⁶, T.P. Kokott³, S. Komamiya²⁴, R. Kowalewski⁸, T. Kress¹¹, P. Krieger⁶, J. von Krogh¹¹, P. Kyberd¹³, G.D. Lafferty¹⁶, H. Lafoux²¹, R. Lahmann¹⁷, W.P. Lai¹⁹, D. Lanske¹⁴, J. Lauber¹⁵, J.G. Layter⁴, A.M. Lee³¹, E. Lefebvre¹⁸, D. Lellouch²⁶, J. Letts², L. Levinson²⁶, C. Lewis¹⁵, S.L. Lloyd¹³, F.K. Loebinger¹⁶, G.D. Long¹⁷, B. Lorazo¹⁸, M.J. Losty⁷, J. Ludwig¹⁰, A. Luig¹⁰, A. Malik²¹, M. Mannelli⁸, S. Marcellini², C. Markus³, A.J. Martin¹³, J.P. Martin¹⁸, G. Martinez¹⁷, T. Mashimo²⁴, W. Matthews²⁵, P. Mättig³, W.J. McDonald³⁰, J. McKenna²⁹, E.A. Mckigney¹⁵, T.J. McMahon¹, A.I. McNab¹³, F. Meijers⁸, S. Menke³, F.S. Merritt⁹, H. Mes⁷, J. Meyer²⁷, A. Michelini⁸, G. Mikenberg²⁶, D.J. Miller¹⁵, R. Mir²⁶, W. Mohr¹⁰, A. Montanari², T. Mori²⁴, M. Morii²⁴, U. Müller³, B. Nellen³, B. Nijjar¹⁶, R. Nisius⁸, S.W. O’Neale¹, F.G. Oakham⁷, F. Odorici², H.O. Ogren¹², N.J. Oldershaw¹⁶, T. Omori²⁴, C.J. Oram^{28,a}, M.J. Oreglia⁹, S. Orito²⁴, M. Palazzo², J. Pálincás³³, F.M. Palmonari², J.P. Pansart²¹, G. Pásztor³², J.R. Pater¹⁶, G.N. Patrick²⁰, M.J. Pearce¹, P.D. Phillips¹⁶, J.E. Pilcher⁹, J. Pinfold³⁰, D.E. Plane⁸, P. Poffenberger²⁸, B. Poli², A. Posthaus³, T.W. Pritchard¹³, H. Przysiezniak³⁰, D.L. Rees¹, D. Rigby¹, M.G. Rison⁵, S.A. Robins¹³, N. Rodning³⁰, J.M. Roney²⁸, E. Ros⁸, A.M. Rossi², M. Rosvick²⁸, P. Routenburg³⁰, Y. Rozen⁸, K. Runge¹⁰, O. Runolfsson⁸, D.R. Rust¹², R. Rylko²⁵, E.K.G. Sarkisyan²³, M. Sasaki²⁴, C. Sbarra², A.D. Schaile⁸, O. Schaile¹⁰, F. Scharf³, P. Scharff-Hansen⁸, P. Schenk⁴, B. Schmitt³, M. Schröder⁸, H.C. Schultz-Coulon¹⁰, M. Schulz⁸, P. Schütz³, J. Schwiening³, W.G. Scott²⁰, T.G. Shears¹⁶, B.C. Shen⁴, C.H. Shepherd-Themistocleous²⁷, P. Sherwood¹⁵, G.P. Sioli², A. Sittler²⁷, A. Skillman¹⁵, A. Skuja¹⁷, A.M. Smith⁸, T.J. Smith²⁸, G.A. Snow¹⁷, R. Sobie²⁸, S. Söldner-Rembold¹⁰, R.W. Springer³⁰, M. Sproston²⁰, A. Stahl³, M. Starks¹², C. Stegmann¹⁰, K. Stephens¹⁶, J. Steuerer²⁸, B. Stockhausen³, D. Strom¹⁹, F. Strumia⁸, P. Szymanski²⁰, R. Tafirout¹⁸, H. Takeda²⁴, P. Taras¹⁸, S. Tarem²², M. Tecchio⁸, N. Tesch³, M.A. Thomson⁸, E. von Törne³, S. Towers⁶, M. Tscheulin¹⁰, T. Tsukamoto²⁴, E. Tsur²³, A.S. Turcot⁹, M.F. Turner-Watson⁸, P. Utzat¹¹, R. Van Kooten¹², G. Vasseur²¹, P. Vikas¹⁸, M. Vincter²⁸, E.H. Vokurka¹⁶, F. Wäckerle¹⁰, A. Wagner²⁷, D.L. Wagner⁹,

C.P. Ward⁵, D.R. Ward⁵, J.J. Ward¹⁵, P.M. Watkins¹, A.T. Watson¹, N.K. Watson⁷, P. Weber⁶,
P.S. Wells⁸, N. Wermes³, B. Wilkens¹⁰, G.W. Wilson²⁷, J.A. Wilson¹, T. Wlodek²⁶, G. Wolf²⁶,
S. Wotton¹¹, T.R. Wyatt¹⁶, S. Xella², S. Yamashita²⁴, G. Yekutieli²⁶, V. Zacek¹⁸,

¹School of Physics and Space Research, University of Birmingham, Birmingham B15 2TT, UK

²Dipartimento di Fisica dell' Università di Bologna and INFN, I-40126 Bologna, Italy

³Physikalisches Institut, Universität Bonn, D-53115 Bonn, Germany

⁴Department of Physics, University of California, Riverside CA 92521, USA

⁵Cavendish Laboratory, Cambridge CB3 0HE, UK

⁶ Ottawa-Carleton Institute for Physics, Department of Physics, Carleton University, Ottawa, Ontario K1S 5B6, Canada

⁷Centre for Research in Particle Physics, Carleton University, Ottawa, Ontario K1S 5B6, Canada

⁸CERN, European Organisation for Particle Physics, CH-1211 Geneva 23, Switzerland

⁹Enrico Fermi Institute and Department of Physics, University of Chicago, Chicago IL 60637, USA

¹⁰Fakultät für Physik, Albert Ludwigs Universität, D-79104 Freiburg, Germany

¹¹Physikalisches Institut, Universität Heidelberg, D-69120 Heidelberg, Germany

¹²Indiana University, Department of Physics, Swain Hall West 117, Bloomington IN 47405, USA

¹³Queen Mary and Westfield College, University of London, London E1 4NS, UK

¹⁴Technische Hochschule Aachen, III Physikalisches Institut, Sommerfeldstrasse 26-28, D-52056 Aachen, Germany

¹⁵University College London, London WC1E 6BT, UK

¹⁶Department of Physics, Schuster Laboratory, The University, Manchester M13 9PL, UK

¹⁷Department of Physics, University of Maryland, College Park, MD 20742, USA

¹⁸Laboratoire de Physique Nucléaire, Université de Montréal, Montréal, Quebec H3C 3J7, Canada

¹⁹University of Oregon, Department of Physics, Eugene OR 97403, USA

²⁰Rutherford Appleton Laboratory, Chilton, Didcot, Oxfordshire OX11 0QX, UK

²¹CEA, DAPNIA/SPP, CE-Saclay, F-91191 Gif-sur-Yvette, France

²²Department of Physics, Technion-Israel Institute of Technology, Haifa 32000, Israel

²³Department of Physics and Astronomy, Tel Aviv University, Tel Aviv 69978, Israel

²⁴International Centre for Elementary Particle Physics and Department of Physics, University of Tokyo, Tokyo 113, and Kobe University, Kobe 657, Japan

²⁵Brunel University, Uxbridge, Middlesex UB8 3PH, UK

²⁶Particle Physics Department, Weizmann Institute of Science, Rehovot 76100, Israel

²⁷Universität Hamburg/DESY, II Institut für Experimental Physik, Notkestrasse 85, D-22607 Hamburg, Germany

²⁸University of Victoria, Department of Physics, P O Box 3055, Victoria BC V8W 3P6, Canada

²⁹University of British Columbia, Department of Physics, Vancouver BC V6T 1Z1, Canada

³⁰University of Alberta, Department of Physics, Edmonton AB T6G 2J1, Canada

³¹Duke University, Dept of Physics, Durham, NC 27708-0305, USA

³²Research Institute for Particle and Nuclear Physics, H-1525 Budapest, P O Box 49, Hungary

³³Institute of Nuclear Research, H-4001 Debrecen, P O Box 51, Hungary

^aAlso at TRIUMF, Vancouver, Canada V6T 2A3

^b Royal Society University Research Fellow

^c Institute of Nuclear Research, Debrecen, Hungary

1 Introduction

The production of Υ mesons¹ in Z^0 decays is highly suppressed. The formation of Υ mesons from the b quarks produced directly in Z^0 decays requires the emission of highly energetic gluons. Alternatively, Υ formation involving the production of $b\bar{b}$ pairs from gluons is suppressed by the large b-quark mass. At present, only an upper limit exists [1]. The interest of these rare decays is increased by the observation at the Tevatron of Υ rates much larger than expected [2], and the subsequent attempt to explain the discrepancy between theory and experimental data by the novel ‘colour-octet’ production models [3]. Υ production in Z^0 decays allows a non-trivial test of these models.

Initially, only ‘colour-singlet’ models were considered theoretically to estimate the production of Υ mesons. In Z^0 decays, the ‘colour-singlet’ fragmentation processes are the ‘b-quark fragmentation’ [4], the ‘gluon fragmentation’ [5] and the ‘gluon radiation’ process [6] (see Fig. 1). The corresponding production rates have been calculated using perturbative QCD and are found to be very small. According to these calculations the ‘b-quark fragmentation’ process is dominant, with a branching ratio of [7]:

$$Br(Z^0 \rightarrow \Upsilon + X) = 1.6 \times 10^{-5},$$

after adding the three lowest Υ bound states and taking into account the contribution of cascade decays from χ_b resonances. In the alternative ‘colour-octet’ models, introduced to explain the Tevatron data, Υ mesons are first produced in a ‘colour-octet’ state and then evolve non-perturbatively into ‘colour-singlet’ states by emission of soft gluons. These ‘colour-octet’ models predict larger Υ production rates in Z^0 decays. According to [7], the dominant process is in this case the ‘gluon fragmentation’ process (see Fig. 1), with a branching ratio of:

$$Br(Z^0 \rightarrow \Upsilon + X) = 4.1 \times 10^{-5},$$

including again the three lowest bound states and cascade decays. These QCD calculations might have, however, large uncertainties since they include only the leading term and higher order corrections could be important. In the case of ‘colour-octet’ models, the total rate depends in addition on free parameters adjusted to the Tevatron data. The validity of these production models and rates has yet to be confirmed by experimental measurements.

In this paper, a search for Υ mesons in Z^0 decays is performed. Υ mesons are identified from their decays into e^+e^- and $\mu^+\mu^-$ pairs. These decays provide a clear signature, since the e^+e^- and $\mu^+\mu^-$ background with invariant mass around 10 GeV/ c^2 is expected to be small. The outline of this paper is as follows: a brief description of the OPAL detector is presented in Section 2, the main selection criteria are described in Section 3, the composition of the background and final selection criteria are discussed in Section 4, and finally, the $Z^0 \rightarrow \Upsilon + X$ branching ratio is obtained in Section 5.

2 The OPAL Detector

The OPAL detector has been described elsewhere [8]. The analysis presented here is based on information from the central tracking system, the lead glass electromagnetic calorimeter and its presampler, the hadron calorimeter and the muon chambers. The tracking system consists of a two layer silicon microstrip vertex detector [9], a vertex drift chamber, a jet chamber and a set of z -chambers for measurements in the z direction (z is the coordinate parallel to the beam axis), all enclosed by a solenoidal magnet coil which produces an axial field of 0.435 T. The main tracking detector is the jet chamber, which has a length of 4 m, a diameter of 3.7 m and which provides up to 159 space points and close to 100% track-finding efficiency for charged tracks in the region $|\cos\theta| < 0.92$, where θ is the polar angle. The momentum resolution in the $r - \phi$ plane can be parametrised as $(\sigma_{p_t}/p_t)^2 = (0.02)^2 + (0.0015 \cdot p_t)^2$, with p_t in GeV/ c . The jet chamber is also able to perform particle

¹In the following Υ refers to any of the three lowest bound states: $\Upsilon(1S)$, $\Upsilon(2S)$ and $\Upsilon(3S)$.

identification by energy loss (dE/dx) measurements with a resolution of 3.5% for minimum ionising particles with the maximum number of ionisation samples [10].

3 Event, lepton and Υ selection

The initial event sample consisted of hadronic Z^0 decays selected using standard OPAL criteria [11]. Tracks were required to satisfy minimum quality cuts as in [12] and only events with at least 7 good quality tracks were considered. The selection efficiency for multihadronic events is $(98.1 \pm 0.5)\%$, with a background contamination smaller than 0.1%. After all cuts, a total of 3.7 million hadronic events were selected.

A sample of 4 million Monte Carlo (MC) simulated multihadronic events (not containing Υ states) was used to study the background. Samples of 2000 MC events simulating each of the processes (see Fig. 1) $Z^0 \rightarrow \Upsilon b\bar{b}$, $Z^0 \rightarrow \Upsilon q\bar{q}gg$, $Z^0 \rightarrow \Upsilon gg$, $Z^0 \rightarrow \Upsilon q\bar{q}$ and $Z^0 \rightarrow \Upsilon g$, were used to estimate the corresponding selection efficiencies. In all these processes, the partons were generated using the corresponding differential cross-sections provided in [4, 5, 6, 7]. In the first three processes, Υ mesons are produced in a ‘colour-singlet’ state and in the last two processes, in a ‘colour-octet’ state. Since ‘colour-octet’ states recombine into colour-singlet states by soft gluon emission, some extra energy is expected around ‘colour-octet’ states. This extra energy has been neglected in the simulation, but the consequences of this approximation are discussed later. For all MC samples, the parton shower and hadronisation processes were simulated using the JETSET model [13], with parameter settings as described in [14]. All these samples were processed using the complete OPAL detector simulation program [15].

Lepton candidates were required to satisfy the following acceptance cuts:

- $p > 3 \text{ GeV}/c$, where p is the track momentum.
- $|\cos\theta| < 0.95$, where θ is the polar angle with respect to the electron beam direction.

In order to ensure sufficient track quality for the calculation of the invariant mass, an accurate polar angle measurement (z chamber association or presampler match, for barrel tracks, and constraint to the point where the track leaves the jet chamber, in the case of forward tracks) was required for all lepton tracks. An additional requirement that at least 10 hits were used for the calculation of the ionisation energy loss eliminates tracks too close to other tracks or to the anode and cathode planes of the jet chamber. Lepton identification with the OPAL detector is described in detail in [12]. The selection requirements used in the present analysis are briefly described below.

The following electron identification requirements were applied:

- $[dE/dx - (dE/dx)_0]/\sigma(dE/dx) > -2.0$, dE/dx being the measured track ionisation energy loss per unit length, $(dE/dx)_0$ the average dE/dx for electrons, and $\sigma(dE/dx)$ the resolution on dE/dx for the candidate track.
- $0.7 < E/p < 1.4$, where E is the electromagnetic energy associated with the track.
- Electrons identified as originating from photon conversions by the algorithm described in [12] were rejected.

The following muon identification requirements were applied [12, 16]:

- A good positional match between an extrapolated track from the central tracking chambers and a reconstructed track segment in the muon chambers. The hadron calorimeter was used outside the regions covered by the muon chambers.

- In order to reduce the background due to kaons decaying to muons or due to hadronic showers penetrating to the muon chambers, muon candidates were required to have a dE/dx measurement consistent with that of a muon. Muon candidates were also rejected if more than 20 muon segments were found within an azimuthal cone of 300 mrad around the candidate segment.

Using simulated events, the efficiencies after acceptance cuts for the above lepton identification selections are $(87.3 \pm 0.9)\%$ and $(81.6 \pm 1.0)\%$ for electrons and muons from Υ decays, respectively, the errors being only statistical.

Υ candidates were selected by demanding a pair of electron or muon tracks with opposite charge, with opening angle $\alpha < 90^\circ$ (in order to reject lepton pairs from opposite jets), and with decay length $L < 1.5$ mm and significance $|L|/\sigma_L < 4$, where σ_L is the error in L (in order to reject lepton pairs from semileptonic decays of heavy quarks²). The decay length is first obtained as the distance in the xy plane between the beam spot and the reconstructed dilepton decay vertex using the direction of the Υ momentum vector as a constraint. This two-dimensional length is then converted into three dimensions using the polar angle of the reconstructed Υ .

4 Background reduction and Υ candidates

The lepton pair invariant mass distribution obtained after all preceding selection cuts is displayed in Fig. 2. In order to increase the sensitivity to Υ mesons, additional background suppression is required.

The following background sources have been considered:

- fake lepton pairs, produced in multihadronic events when one or both tracks are hadrons misidentified as leptons,
- genuine lepton pairs, which result at high invariant mass mainly from semi-leptonic decays of independent heavy hadrons, and finally
- four-fermion events, namely the process $e^+e^- \rightarrow q\bar{q} + \ell^+\ell^-$, where the $\ell^+\ell^-$ pair results mainly from a virtual photon emission [17].

The first two background sources (multihadronic background) can be estimated by counting the number of ‘wrong lepton’ pairs ($e^\pm\mu^\mp$), since there is no correlation between the lepton types. As seen in Fig. 2, these ‘wrong lepton’ pairs provide a good description of the background, except at the position of the J/ψ peak, where a signal is observed, as expected. The third background source (four-fermion background) can only be estimated using simulated events (see below).

The origin of the multihadronic background was studied using the sample of 4 million simulated events described before. According to the simulation, the background for invariant masses above $5 \text{ GeV}/c^2$ consists mainly of genuine lepton pairs produced by heavy quark pairs in events with hard gluon radiation, or by heavy quark pairs produced by gluon splitting. In order to reduce the multihadronic background the following additional requirement (isolation cut) was applied: the extra energy, E_{isol} (sum of track momenta and energy of electromagnetic clusters not associated to tracks), within a pair of cones with a half-angle of 35° around the direction of each lepton was required to be smaller than 8 GeV. The lepton pair invariant mass distribution after this cut is shown in Fig. 3. For masses above $5 \text{ GeV}/c^2$, the multihadronic background is completely suppressed by the isolation cut, as shown by the distribution of $e^\pm\mu^\mp$ pairs. By performing a linear extrapolation of the number of $e^\pm\mu^\mp$ pairs obtained as a function of the E_{isol} cut, the hadronic background in the region 5–15 GeV/c^2 is estimated to be 0.7 ± 0.5 events. This background is distributed as follows: 0.5 ± 0.5 events in the region 5–8 GeV/c^2 , 0.1 ± 0.1 events in the region 8–11 GeV/c^2 , and 0.1 ± 0.1 events in the region 11–15 GeV/c^2 .

²The Υ are expected to originate from the primary vertex.

The four-fermion background was estimated using the generator FERMISV [18]. The simulated event sample was equivalent to 12 times the sample expected in the OPAL data. After scaling, the expected background from four-fermion events in the multihadronic data sample is 4.7 ± 0.5 events in the region $5\text{--}15 \text{ GeV}/c^2$. This background is distributed as follows: 2.3 ± 0.4 events in the region $5\text{--}8 \text{ GeV}/c^2$, 1.5 ± 0.3 events in the region $8\text{--}11 \text{ GeV}/c^2$, and 0.9 ± 0.2 events in the region $11\text{--}15 \text{ GeV}/c^2$. The uncertainties on these MC predictions are mainly statistical, since the theoretical error is of the order of 5% [17]. The contribution to the number of dilepton pairs due to the production of $b\bar{b}$ resonances by virtual photons (not included in the Monte Carlo) has been estimated as in [17]. The result is 0.005 events in the region $5\text{--}15 \text{ GeV}/c^2$ and this dilepton source can therefore be neglected.

According to the simulation, 90% of the lepton pairs from $\Upsilon(1S)$ decays have an invariant mass in the range $8\text{--}11 \text{ GeV}/c^2$ (for $\Upsilon(2S)$ and $\Upsilon(3S)$ the result is 93%). In the following, this invariant mass range (signal region) is used to determine the background and calculate the Υ selection efficiency. As shown in Fig. 3, there are 13 pairs with invariant mass between 5 and 15 GeV/c^2 , 8 of them in the signal region. Some properties of these eight Υ candidates are listed in Table 1. The 5 pairs above $5 \text{ GeV}/c^2$, but outside the signal region, agree well with the expected 3.8 ± 0.7 background events from four-fermion and hadronic processes. Since in the signal region the background is 1.6 ± 0.3 events, the ‘background-subtracted’ number of Υ candidates is:

$$N_{\Upsilon} = N_{\text{cand}} - N_{\text{bkg}} = 6.4 \pm 2.8 \pm 0.3,$$

where the first error is statistical and the second results from the background uncertainty. The probability that the background fluctuates to the observed signal is 4×10^{-4} .

Event	Mass (GeV/c^2)	$p_{\ell^+\ell^-}$ (GeV/c)	$\cos \alpha$	L/σ_L	E_{isol} (GeV)
$\mu^+\mu^-$	8.46 ± 0.18	30.6	0.84	0.19	0.0
$\mu^+\mu^-$	9.06 ± 0.23	33.5	0.82	-1.10	7.9
$\mu^+\mu^-$	9.78 ± 0.18	18.4	0.55	0.38	6.7
$\mu^+\mu^-$	9.87 ± 0.24	25.1	0.72	0.05	3.6
$\mu^+\mu^-$	10.57 ± 0.18	18.6	0.48	-0.70	0.0
e^+e^-	8.64 ± 0.31	33.0	0.85	0.88	0.0
e^+e^-	8.64 ± 0.21	29.0	0.80	-0.67	0.6
e^+e^-	9.68 ± 0.17	9.8	0.01	-3.38	6.5

Table 1: *Some properties of the Υ candidates. The invariant mass error is calculated for each candidate from the expected errors on individual track parameters.*

5 Inclusive branching ratio

The three lowest Υ bound states are expected to be produced in Z^0 decays, but their relative abundances depend on the production mechanism. If the Υ yield is dominated by direct production rather than cascade decays of χ_b states, $\Upsilon(1S)$, $\Upsilon(2S)$ or $\Upsilon(3S)$ states are expected to be produced in the proportions 1:0.5:0.5 [7]. Other hypotheses are considered later for error calculation purposes. Since the average experimental invariant mass resolution σ_M is about $210 \text{ MeV}/c^2$, no clear discrimination between the different states is possible (see Table 2). In addition, according to the simulation, the peak of the invariant mass distribution of e^+e^- pairs is shifted by about $300 \text{ MeV}/c$ and has a large tail towards low masses, due to the energy loss by bremsstrahlung in the detector. About 30% of e^+e^- pairs have masses more than $3\sigma_M$ below the nominal Υ mass. Another energy loss effect, due to the

radiative decay process $\Upsilon(1S) \rightarrow \ell^+ \ell^- \gamma$, has been calculated using QED as in [20], and is included in the simulation.

State	Mass (GeV/c ²)	$Br(\Upsilon \rightarrow e^+e^-)$ (in %)	$Br(\Upsilon \rightarrow \mu^+\mu^-)$ (in %)	$Br(\Upsilon(3S) \rightarrow \Upsilon + X)$ (in %)	$Br(\Upsilon(2S) \rightarrow \Upsilon + X)$ (in %)
$\Upsilon(1S)$	9.460	2.52 ± 0.17	2.48 ± 0.07	11.7 ± 0.5	31.1 ± 1.6
$\Upsilon(2S)$	10.023	not measured	1.31 ± 0.21	10.6 ± 0.8	–
$\Upsilon(3S)$	10.355	not measured	1.81 ± 0.17	–	–

Table 2: *Some properties of Υ states, as given in the Review of Particle Properties [19].*

In order to calculate the Z^0 branching ratio to inclusive Υ states, the selection efficiency ϵ_Υ must be known. This efficiency, however, depends on the production process, as can be seen in Table 3. This dependence is introduced in particular by the isolation cut. The Z^0 branching ratio to inclusive Υ states is calculated as follows:

$$Br(Z^0 \rightarrow \Upsilon + X) = \frac{N_\Upsilon}{N_{\text{had}}} \cdot \frac{\epsilon_{\text{had}}}{\epsilon_\Upsilon} \cdot \frac{R_{\text{had}}}{2Br(\Upsilon \rightarrow \ell^+ \ell^-)},$$

where N_Υ is the number of Υ candidates after background subtraction, N_{had} is the number of hadronic events, $\epsilon_{\text{had}} = 0.981 \pm 0.005$ is the multihadronic selection efficiency, $R_{\text{had}} = 0.699 \pm 0.003$ [19] is the Z^0 hadronic branching ratio, and $Br(\Upsilon \rightarrow \ell^+ \ell^-) = (2.31 \pm 0.16)\%$, where $\ell = \mu$ or e , is the average effective Υ leptonic branching ratio. This effective leptonic branching ratio has been calculated assuming that $\Upsilon(1S)$, $\Upsilon(2S)$ and $\Upsilon(3S)$ are produced with relative abundances 1:0.5:0.5, and taking into account the contribution of cascade decays between the various Υ states (see Table 2). It has also been assumed that the electron and muon leptonic branching ratios of the Υ states are equal. For each model the measured and theoretically predicted Z^0 branching ratios to inclusive Υ states are reported in Table 3. It is noted that, except for the gluon fragmentation model into ‘colour-octet’ Υ states, $Z^0 \rightarrow \Upsilon q\bar{q}$, the measured branching ratios are much larger than theoretical expectations. The average efficiency, obtained by weighting individual efficiencies according to the theoretically expected rates, is $\epsilon_\Upsilon = 0.249$. This efficiency is used in the following to calculate the Z^0 branching ratio to inclusive Υ states.

Production process	Efficiency no isolation cut	Efficiency isolation cut	$Br(Z^0 \rightarrow \Upsilon + X)$ measured	$Br(Z^0 \rightarrow \Upsilon + X)$ expected
$Z^0 \rightarrow \Upsilon b\bar{b}$	0.398 ± 0.011	0.246 ± 0.010	$(1.1 \pm 0.5) \times 10^{-4}$	1.6×10^{-5} [7]
$Z^0 \rightarrow \Upsilon q\bar{q}g$	0.311 ± 0.010	0.174 ± 0.010	$(1.4 \pm 0.6) \times 10^{-4}$	0.7×10^{-6} [5]
$Z^0 \rightarrow \Upsilon g$	0.328 ± 0.011	0.211 ± 0.009	$(1.2 \pm 0.5) \times 10^{-4}$	0.5×10^{-6} [6]
$Z^0 \rightarrow \Upsilon q\bar{q}$	0.355 ± 0.011	0.252 ± 0.010	$(1.0 \pm 0.4) \times 10^{-4}$	4.1×10^{-5} [7]
$Z^0 \rightarrow \Upsilon g$	0.376 ± 0.011	0.376 ± 0.011	$(0.7 \pm 0.3) \times 10^{-4}$	1.0×10^{-6} [7]

Table 3: *Monte Carlo calculation of Υ selection efficiencies for the various production models. For each model the measured and the expected Z^0 branching ratio to inclusive Υ states are reported. The error on the measured value is only statistical.*

The following systematic uncertainties have been considered (see Table 4):

- The uncertainty related to the background subtraction was determined as described above.
- The uncertainty related to the lepton identification efficiency and track quality cuts was determined from data samples as in [20].

- The resolutions predicted by the detector simulation for track parameters in $r-\phi$ (track curvature κ , distance of closest approach to the coordinate origin d_0 , and azimuthal angle at the point of closest approach ϕ_0) and in z (tangent of the dip angle $\tan \lambda$ and the z -coordinate at the point of closest approach z_0) were adjusted to describe the data. These track parameter resolutions were varied by 10% in $r-\phi$ and 30% in z to obtain the corresponding systematic error in the efficiency.
- The uncertainty on $Br(\Upsilon \rightarrow \ell^+ \ell^-)$ was determined as described above, assuming that the Υ states are produced in the proportions 1:0.5:0.5. If Υ states are produced with relative abundances 1:1:1, the effective leptonic branching ratio differs by 1.7% (relative difference to the central value). This difference has been added in quadrature to obtain the total uncertainty on $Br(\Upsilon \rightarrow \ell^+ \ell^-)$.
- Since the parameters used to calculate the Υ production yield in ‘colour-octet’ models are adjusted to the Tevatron data, there are still uncertainties concerning the composition of the Υ sample. If Υ production is dominated by cascade decays of χ_b states, a softer Υ spectrum is expected. According to the simulated events, the selection efficiency would be smaller by 4.8% in this case. This value is used to account for uncertainties in the Υ momentum spectrum.
- The Υ selection efficiency has been calculated assuming that Υ mesons decay isotropically. In order to account for the unknown Υ polarization, the efficiency has been recalculated, as in [2], assuming that the angular distribution of leptons from Υ decays in the Υ rest frame is proportional to $1 + \cos^2 \theta^*$, where θ^* is the emission angle. The corresponding change in efficiency is 7.1%.
- As discussed in Section 3, the soft gluon energy emitted by ‘colour-octet’ Υ states in order to recombine into ‘colour-singlet’ states has been neglected in the MC simulation. This energy affects the E_{isol} calculation. According to the MC, the average E_{isol} energy is 1.7 GeV. The difference between this value and the average value of 3.2 ± 1.3 GeV obtained from the eight Υ candidates (see Table 1) has been used as an estimator of this extra energy. The change in efficiency obtained by adding in the simulation this extra energy to E_{isol} is 5.2%.

Error source	Contribution
background uncertainty	4.7 %
lepton identification	4.5 %
track parameter resolution	2.4 %
$Br(\Upsilon \rightarrow \ell^+ \ell^-)$	7.1 %
Υ momentum spectrum	4.8 %
Υ polarization	7.1 %
E_{isol} calculation	5.2 %
MC statistics	4.1 %
Total systematic error	14.7 %

Table 4: *Summary of relative systematic uncertainties on the inclusive Υ production rate.*

Taking into account the total systematic uncertainty, the branching ratio of Z^0 into inclusive Υ states is:

$$Br(Z^0 \rightarrow \Upsilon + X) = (1.0 \pm 0.4 \pm 0.1) \times 10^{-4},$$

where the first error is statistical and the second systematic. This branching ratio is compatible with the theoretical expectation of 5.9×10^{-5} , obtained by adding all production mechanisms. Taking

into account systematic errors, the expected number of events using this theoretical ratio is 5.3 ± 0.5 , including background events. The probability that this expected number fluctuates to the observed number of 8 events is 17%. The branching ratio for ‘colour-singlet’ models alone (1.7×10^{-5}) is in contrast too small to explain the observed number of events, as was the case at the Tevatron [3]. The expected number of events is in this case 2.7 ± 0.3 , and the probability that this number fluctuates to the observed number of events is 0.8%. Further properties of the events are discussed below.

A search for displaced vertices with significance $L/\sigma_L > 3$ was performed using the eight Υ candidates. The algorithm to reconstruct the vertices is described in [21]. According to the MC simulated events, the efficiency of this algorithm to identify an event of the type $Z^0 \rightarrow \Upsilon b\bar{b}$, where two additional b-quarks are produced, is 60%. If all Υ events observed in the data are produced by this mechanism, 4.0 data events are expected to be identified by the b-quark tagging algorithm, but no event is found. The probability of this fluctuation is 1.8% and an upper limit of 0.7×10^{-4} at 90% CL is obtained for $Br(Z^0 \rightarrow \Upsilon b\bar{b})$. All other production mechanisms are consistent with the observed number of displaced vertices. Similarly, if the production mechanism $Z^0 \rightarrow \Upsilon g$ is responsible for all Υ events observed in the data, 6.2 Υ candidates are expected to be found with momenta above 40 GeV/c², but no candidate is observed in this momentum region (see Table 1). The probability of this fluctuation is 0.2%, and an upper limit of 0.3×10^{-4} at 90% CL is obtained for $Br(Z^0 \rightarrow \Upsilon g)$. The momentum distribution of the Υ candidates is consistent with all other production mechanisms.

It is noted that the production mechanisms $Z^0 \rightarrow \Upsilon b\bar{b}$ and $Z^0 \rightarrow \Upsilon g$ cannot explain all the observed events, but it cannot be excluded that they contribute partially to the total signal. Furthermore, the large branching ratio observed in the data suggests that the observed signal could result from the contribution of several mechanisms. Since the statistics are insufficient to proceed to further tests of the various models, an additional error of 18% is included to account for uncertainties in the production mechanism. This error is calculated as the r.m.s. spread of the branching ratios for the various production models. The $Z^0 \rightarrow \Upsilon g$ model has been excluded from the calculation, since both the theoretical branching ratio and the momentum analysis indicate that its contribution to the total signal is likely to be small. The measured decay ratio of Z^0 into inclusive Υ states is then,

$$Br(Z^0 \rightarrow \Upsilon + X) = (1.0 \pm 0.4 \pm 0.1 \pm 0.2) \times 10^{-4},$$

where the first error is statistical, the second systematic and the third error accounts for the uncertainty in the production mechanism. This measured branching ratio is compatible with the upper limit obtained by DELPHI [1].

6 Summary

The production of Υ mesons in hadronic Z^0 decays is studied using a sample of 3.7 million hadronic Z^0 decays. Υ mesons are identified from their decays into e^+e^- and $\mu^+\mu^-$ pairs. Eight candidates are found over an estimated background of 1.6 ± 0.3 events. The probability that the background fluctuates to the observed signal is 4×10^{-4} .

Assuming that the dominant production mechanism is gluon fragmentation into ‘colour-octet’ Υ states, the following measurement for the inclusive branching ratio into the three lightest Υ states is obtained:

$$Br(Z^0 \rightarrow \Upsilon + X) = (1.0 \pm 0.4 \pm 0.1 \pm 0.2) \times 10^{-4},$$

where the first error is statistical, the second systematic and the third error is obtained after consideration of other possible production mechanisms. The measured ratio agrees within errors with the expected theoretical ratio, after including both ‘colour-singlet’ and ‘colour-octet’ production mechanisms.

Acknowledgements

It is a pleasure to thank the SL Division for the efficient operation of the LEP accelerator, the precise information on the absolute energy, and their continuing close cooperation with our experimental group. In addition to the support staff at our own institutions we are pleased to acknowledge the Department of Energy, USA, National Science Foundation, USA, Particle Physics and Astronomy Research Council, UK, Natural Sciences and Engineering Research Council, Canada, Fussesfeld Foundation, Israel Ministry of Science, Israel Science Foundation, administered by the Israel Academy of Science and Humanities, Minerva Gesellschaft, Japanese Ministry of Education, Science and Culture (the Monbusho) and a grant under the Monbusho International Science Research Program, German Israeli Bi-national Science Foundation (GIF), Direction des Sciences de la Matière du Commissariat à l'Energie Atomique, France, Bundesministerium für Forschung und Technologie, Germany, National Research Council of Canada, Hungarian Foundation for Scientific Research, OTKA T-016660, and OTKA F-015089.

References

- [1] DELPHI Collab., P.Abreu et al., *Search for promptly produced heavy quarkonium states in hadronic Z decays*, CERN-PPE/95-145, submitted to Z. Phys. **C**.
- [2] CDF Collab., F.Abe et al., *Υ production in $p\bar{p}$ collisions at $\sqrt{s} = 1.8$ TeV*, FERMILAB-PUB-95/271-E, submitted to Phys. Rev. Lett.
- [3] M.Cacciari et al., Phys. Rev. Lett. **73** (1994) 1586;
M.Cacciari et al., Phys. Lett. **B356** (1995) 553;
P.Cho and A.Leibovich, *Color-Octet quarkonia production*, CALT 68-1988, to be published in Phys. Rev. **D**.
- [4] E.Braaten, K.Cheung, T.C.Yuan, Phys. Rev. **D48** (1993) 4230;
V.Barger, K.Cheung, and W.Y.Keung, Phys. Rev. **D41** (1990) 1541.
- [5] E.Braaten, T.C.Yuan, Phys. Rev. Lett. **71** (1993) 1673;
K.Hagiwara, et al., Phys. Lett. **B267** (1991) 527, Erratum: Phys. Lett. **B316** (1993) 631.
- [6] K.J.Abraham, Z. Phys. **C44** (1989) 467;
J.H.Kühn and H.Schneider, Z. Phys. **C11** (1981) 263;
W.Y.Keung, Phys. Rev. **D23** (1981) 2072.
- [7] P.Cho, *Prompt Upsilon and Psi Production at LEP*, CALT-68-2020.
- [8] OPAL Collab., K.Ahmet et al., Nucl. Instrum. and Meth. **A305** (1991) 275.
- [9] P.Allport et al., Nucl. Instrum. and Meth. **A324** (1993) 34;
P.Allport et al., Nucl. Instrum. and Meth. **A346** (1994) 476.
- [10] M.Hauschild et al., Nucl. Instrum. and Meth. **A314** (1992) 74.
- [11] OPAL Collab., G.Alexander et al., Z. Phys. **C52** (1991) 175.
- [12] OPAL Collab., P.Acton et al., Z. Phys. **C58** (1993) 523.
- [13] T.Sjöstrand, Comp. Phys. Comm. **82** (1994) 74;
T.Sjöstrand, JETSET 7.4 Manual, CERN-TH.7112/93.
- [14] OPAL Collab., G.Alexander et al., *A Comparison of b and uds quark jets to gluon jets*, CERN-PPE/95-126, to be published in Z. Phys. **C**.
- [15] J.Allison et al., Nucl. Instrum. and Meth. **A317** (1991) 47.
- [16] OPAL Collab., R.Akers et al., Z. Phys. **C60** (1993) 199.
- [17] L3 Collab., A.Adam et al., Phys. Lett. **B321** (1994) 283;
ALEPH Collab., D.Buskulic et al., Z. Phys. **C66** (1995) 3.
- [18] J.M.Hilgart, R.Kleiss and F.Le Diberder, Comp. Phys. Comm. **75** (1993) 191.
- [19] L.Montanet et al., Review of Particle Properties, Phys. Rev. **D50** (1994) 1173.
- [20] OPAL Collab., G.Alexander et al., *J/ψ and ψ' production in hadronic Z decays*, CERN-PPE/95-153, submitted to Z. Phys. **C**.
- [21] OPAL Collab., R.Akers et al., Z. Phys. **C66** (1995) 19.

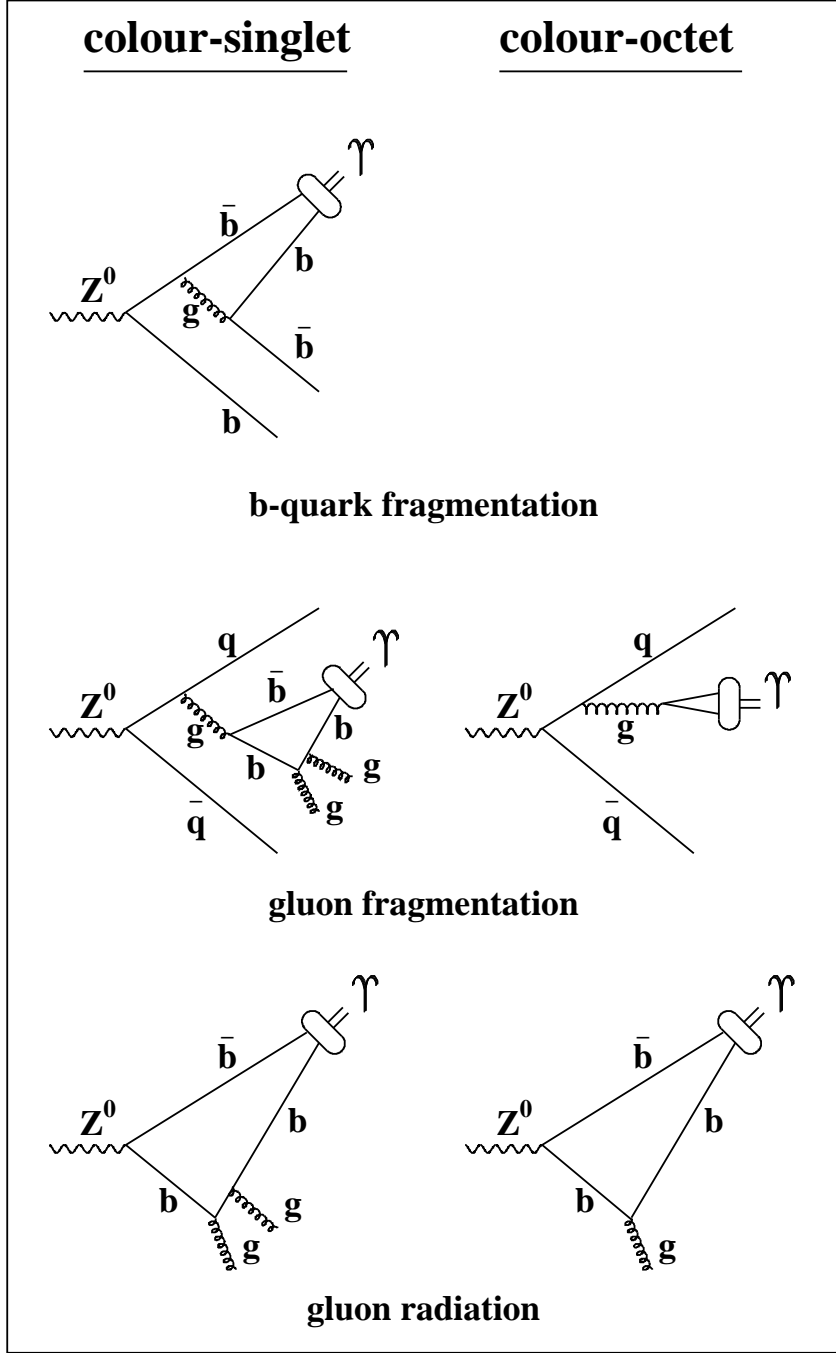


Figure 1: Feynman diagrams for various Υ ‘colour-singlet’ and ‘colour-octet’ production processes.

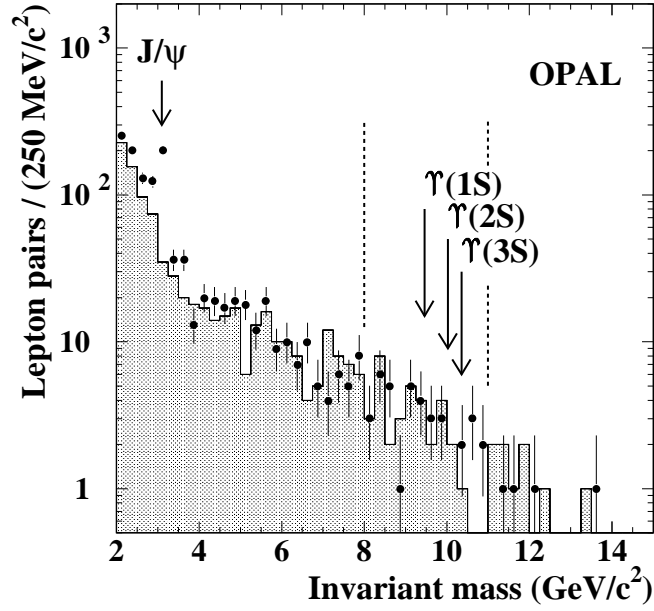


Figure 2: Invariant mass distribution for e^+e^- and $\mu^+\mu^-$ pairs after all cuts except the isolation cut. The expected hadronic background estimated with $e^\pm\mu^\mp$ pairs is shaded.

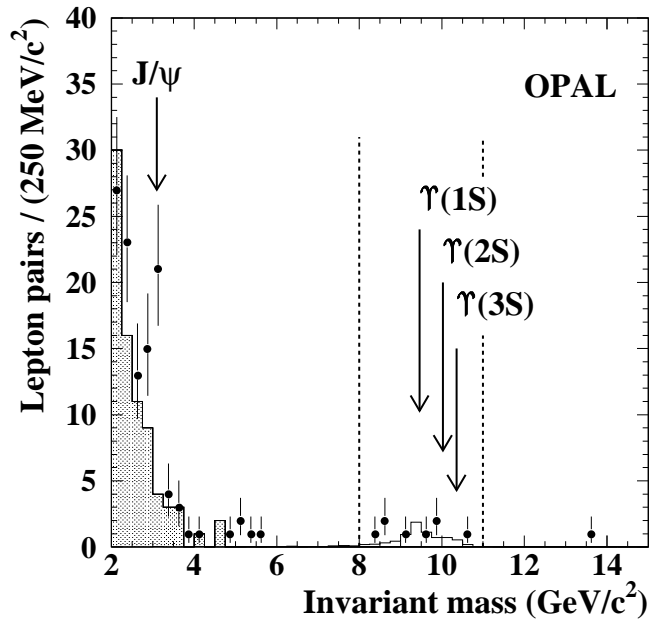


Figure 3: Invariant mass distribution for e^+e^- and $\mu^+\mu^-$ pairs after all cuts. The expected background estimated with $e^\pm\mu^\mp$ pairs is shaded. The solid line in the signal region corresponds to the MC expected distribution for inclusive Υ states.